The 2013 World Congress on
Advances in Structural Engineering and Mechanics (ASEM13)
Jeju, Korea, September 8-12, 2013

Control of vibrations of two metallic structures produced and designed in Portugal - Cantilever highway sign support and Tall lattice wind tower

Fábio Paiva[1)] Jorge Henriques[1)] and *Rui C. Barros[2)]
[1), 2)] *Department of Civil Engineering, FEUP, Porto 4200-465, Portugal*
[2)] rcb@fe.up.pt

ABSTRACT

The present work illustrates a technique for the control of vibrations of two metallic structures produced and designed in Portugal, a cantilever highway sign support and a tall lattice wind tower by recurring to a TMD. A methodology for simulating natural wind histories for in-service behavior of these structures is presented. The study only evaluates the structural response of the cantilevered sign support to natural winds gusts applied on the frontal surface of the signboard (out-plane behavior). In the case of the tall lattice wind tower it was additionally considered that the tower presents the rotor stopped in its most unfavorable position. Concerning the application of TMD, it was concluded that this device is proving to be effective in terms of displacement and acceleration reductions when the structure is subjected to series of artificially generated natural winds.

1. INTRODUCTION

During the past two decades, many structures have shown underlying problems associated with their reduced fatigue performance. Defective welds, aging material, and harsh environmental conditions (particularly wind loading) have exacerbated these problems. In general, highway sign supports and lattice towers must withstand in-service dynamic loads, which constitute the fatigue environment.

The flexibility, combined with low mass, gives to cantilever sign supports low resonant frequencies of about 1 Hz. The damping is extremely low, typically less than 1% of the critical damping. These conditions make cantilevered support structures particularly susceptible to large-amplitude vibration and/or fatigue cracking due to wind loading (Dexter 2005). .Additionally, four wind-loading phenomena were identified as possible sources of large-amplitude vibrations which could lead to fatigue failures (Dexter 2005): galloping, vortex shedding, natural wind gusts, and truck-induced-wind gusts. As it is indicated and summarized in Figure 1, not all of the structures mentioned are affected by all of these phenomena. This change in angle of attack facilitates galloping. Therefore, in cantilevered structures galloping is of primary concern. Vortex shedding in a cantilevered structure has not been reported [5] and will therefore not be discussed in this paper.

	Galloping	Vortex Shedding	Natural Wind	Truck Gusts
Sign	X	*	X	X
Signal	X		X	X
Luminaire		X	X	

Note: X indicates structure is susceptible to this type of loading
* Vortex shedding occurred in an overhead sign bridge

Fig. 1: Susceptibility matrix (Dexter 2005)

The new idea of developing lattice towers of great height, since they have significantly lower construction costs (Henriques 2012), (Henriques 2013), poses new challenges for the structural engineers with regard to dynamic effects. Lattice towers are sensitive to the dynamic environments generated by wind, ice, earthquakes, impact, blast, explosions and mechanical failures of some of their components. The vibrations induced in the tall lattice tower structures by these environmental and mechanical causes cover an ample spectrum of frequencies, which affect the towers in different ways ranging from serviceability problems to fatigue and collapse (Madugula 2002).

To mitigate the dynamic effects can be installed several types of damping devices, one of which is a tuned mass damper (TMD). A TMD consisting of a mass, damping and a spring, is an effective and reliable structural vibration control device commonly attached to a vibrating primary system for suppressing undesirable vibrations induced by machinery as well as by wind and earthquake loads. The natural frequency of the TMD is tuned in resonance with the fundamental mode of the primary structure, so that a large amount of the structural vibrating energy is transferred to the TMD and then dissipated by the damping as the primary structure is subjected to external disturbances. Consequently, the safety and comfort characteristics of the structure are greatly enhanced. The TMD system has been successfully installed in slender skyscrapers and slender towers to suppress the wind-induced structural dynamic responses (Lee 2006).

The following sections details the fundamental wind loads effects on the presented structures. Afterwards the methodology to generate artificial series of wind is presented, taking into account the Method of Shinozuka and the spectral density function given in Eurocode 1-4 (Wind actions) (Eurocode1 2005). A theoretical implementation of TMD will be studied, and a comparative analysis of the structure response (displacements and accelerations) with and without TMD will be made

2. ARTIFICIAL WIND GENERATION

This current section presents the hypothesis under which natural wind was simulated, to create time series acting on the structures. In order to obtain accurate results from the model, the load placed on the structures must be representative of the actual loading scenario. Other than self-weight, most loads applied to the present structures are dynamic in nature. These include but are not limited to wind gusts, ground motion, and vehicle impact (only for the sign support). Dynamic wind loads are the focus of this section because every structure is subjected to them regardless of

location. This section will mainly focus on the effects of natural wind on the structures and the development of the wind loading that is applied to the structural model.
The aim is to model the turbulent nature of wind in the horizontal direction using a simplified model of natural wind as presented by Iannuzzi and Spinelli (Iannuzzi 1987). In order to find an accurate wind velocity the mean and fluctuating components of wind must be added together. This load will be equivalent to a wind time history with a 600 second period and a sample period equal to 0.2 seconds.

2.1 Analytical Simulation of Turbulent-Wind

The wind time history $v(x, y, z, t)$ is the changing value of wind speed with respect to time. When applied to a structure, two components can be considered: a mean component $\bar{U}$ and a fluctuating component $u(x, y, z, t)$, in which x refers to the along-wind direction that will be the only direction analyzed. The fluctuations of wind velocity along time also have a spatial variability, which for a first approximation is herein neglected. This concept can be expressed through the Eq. (1):

$$v(x, y, z, t) = \bar{U}(z) + u(x, y, z, t) \tag{1}$$

2.2 Mean Wind Speed Component

A logarithmic law is used to describe the variation of mean wind speed with elevation above the Earth surface within the atmospheric boundary layer. The logarithmic law is considered slightly more accurate for larger heights but is also more difficult to use (Scanlan 1986).

Taking into consideration Eurocode 1 (EN 1991-1-4), the mean wind velocity varies with height and is defined as the average value of wind speed for a 10 minutes period at an appropriate height above ground. It depends on the terrain roughness and orography and on the basic wind velocity v_b and should be determined according to Eq. (2):

$$\bar{U}(z) = v_m(z) = c_r(z)c_0(z)v_b \tag{2}$$

where $c_r(z)$ is the roughness factor and $c_0(z)$ is the orography factor (usually taken as 1).

The wind action calculated according to the EN 1991-1-4 gives characteristic values which are obtained from base values of wind speed and wind pressure, corresponding to a probability of annual exceedence of 2% (i.e., 0.02); that is equivalent to a return period of 50 years. In some situations it is advantageous to consider a fundamental velocity with a probability of annual exceedence (p) different from 0,02 (or 2%).

The method used by Eurocode 1 is based on the statistical treatment of European wind pressure data. The basic velocity is then obtained multiplying v_b by a probably factor c_{prob} (given below, Eq. (3)) and dependent of the desired or intended probability (p).

$$c_{prob} = \left(\frac{1-k\ln(-\ln(1-p))}{1-k\ln(-\ln(1-0.98))}\right)^n \quad (3)$$

The shape parameter k and the exponent n are parameters that should be quantified in the respective national annexes, and whose recommended values are 0,2 and 0,5 respectively. The shape parameter depends on the coefficient of variation of the extreme-value distribution.

Important assumptions must be made regarding the mean wind velocity at which the sign support structures should be analyzed. It is impractical to forecast the future wind history at each location of the cantilever sign support structures. Therefore the design procedure is based on a spectral analysis using the 10 minutes mean wind velocity, in which was considered a probability of exceedence equal to $p = 50\%$ (c_{prob} =0.77). This latter probability of exceedence represents the in-service dynamic behavior of the structure, when subjected to natural wind gusts with a greater probability of occurrence.

2.3 Turbulent Wind Speed Component

Much research has been done in the past in order to develop a spectrum that can accurately predict the dynamic characteristic of wind. Although the complexity of wind due to its gusty nature can never be predicted, the wind spectra assumes that over a time period the statistical characteristics of wind can be regarded as constant (Davenport 1961).

Firstly it is addressed the methodology for generating time series of wind to be used latter in the calculation of the instantaneous dynamic pressures, and therefore in the quantification of the generalized wind forces.

The methodology used to generate synthetic time series is commonly referred as the Method of Shinozuka that bases the generation of time series in the calculation of the inverse function of the Fourier Transform of the amplitude of the random process (given by a spectral density function of the energy of such process). The generation of synthetic series of wind occurs in the range of wavelengths corresponding to the development of fluctuations of wind velocity with an approximately Gaussian distribution of the atmospheric wind flow.

The purpose of the method is to obtain a realization of a stochastic process (in the present case, a time series of the fluctuations of the longitudinal component of wind velocity) from the spectral density function that characterizes the process (Ferreira 2011).

The method uses this spectral density function to perform a weighted sum of sinusoidal functions (in this case of cosines). The contribution of each of the N waves is given by the amplitude of the spectrum ($S_L(z,n)$, real function) for each corresponding natural frequency (n). The phases are obtained (for the case of one-dimensional spectrum of simple non-correlated series) by pseudo-random number generation in the interval $[0,2\pi]$.

According to the Shinozuka's method in the simplest case of one-dimensional univariate stochastic processes, a realization of the random process may be obtained by Eq. (4):

$$u(t) = \sqrt{2}\sum_{k=1}^{N}\sqrt{S_v(z,n_k)\Delta n}\cos(2\pi n_k t + \phi_k) \quad and\ \Delta n = \frac{n_{max}-n_{min}}{N} \tag{4}$$

Eq. (4) has been used by Iannuzzi and Spinelli (Iannuzzi 1987), and it has been found to generate accurate wind histories when compared to measured wind records. In the previous expression N is the number of frequencies of the spectrum discretization, and n is the frequency. To generate the synthetic time series of wind velocity it is necessary to define a spectral density function of the fluctuations of longitudinal velocity of the wind; the spectral density function given in Eurocode 1 is used herein in the dimensionless form of the following Eq. (5) and (6) (Annex B, of EN 1991-1-4):

$$S_L(z,n_k) = \frac{n_k S_v(z,n_k)}{\sigma_v^2} = \frac{6{,}8 f_L(z,n_k)}{(1+10{,}2 f_L(z,n_k))^{5/3}} \tag{5}$$

$$f_L(z,n_k) = \frac{n_k L(z)}{v_m(z)} \quad and \quad \begin{cases} L(z) = L_t\left(\frac{z}{z_t}\right)^{\alpha} & for \quad z \geq z_{min} \\ L(z) = L(z_{min}) & for \quad z < z_{min} \end{cases} \tag{6}$$

where:

$L(z)$	is the turbulent length scale representing the average gust size for natural winds. For heights z below 200 m the turbulent length scale may be calculated using expression (6). With a reference height of z_t = 200 m and a reference length scale of L_t = 300 m, the power α = 0,67 + 0,05 ln(z_0) where the roughness length z_0 is expressed in m. The minimum height z_{min} is given in Table 4.1 of the Eurocode 1 (EN 1991-1-4).
$S_v(z,n_k)$	is the one-sided variance spectrum;
$f_L(z,n_k)$	is a non-dimensional frequency;
$\sigma_v = k_r v_b k_l$	is the standard deviation of the turbulence;
k_l	is the turbulence factor;
k_r	is the terrain factor.

For the generation of the synthetic series to be considered an ergodic process, according to (Ferreira 2011) the number N of frequencies for discretization of the spectrum should be sufficiently high. Taking into consideration the results in (Ferreira 2011) a value of N=1000 was shown a good compromise. The frequencies n_{min} and n_{max} must be determined accordingly with the f_L limits of power spectral density function of the EC1-4, that way the wind turbulence effect will be clearly characterized. In order for a simulated spectrum to more closely follow the target spectrum, multiple wind histories need to be considered. To illustrate this, ten simulated wind records were generated using the same parameters discussed previously.

2.4 Wind Dynamic Action

For the instantaneous wind velocity $v(t)$ at any height given by the sum of a constant mean component $\overline{U}(z)$ with a dynamic fluctuation component $u(t)$, the instantaneous wind force $F(t)$on any surface A is given by:

$$F(t) = \frac{1}{2}\rho c_f A[(U(z) + u(t)]^2 \tag{7}$$

The fluctuations of wind velocity along time also have a spatial variability, which for the sign support as a first approximation is herein neglected.

For the case tall slender tower under study, whereas the response is majorly due to the contribution of the first mode of vibration (which is also a condition imposed by EC 1-4 for the calculation of the structural factor), modeled as a structural system with one degree of freedom, the passage or conversion of the power spectrum of the wind velocity fluctuations into structural response spectrum is given by Eq. (8):

$$S_X(n) = \frac{4\overline{X}}{\overline{U}^2}.[H(n)]^2.\chi^2(n).S_u(n) \tag{8}$$

where *[H(n)]*^{2} represents the mechanical admittance and $\chi^2(n)$ represents an aerodynamic admittance function [15] given approximately by Eq. (9).

$$\chi(n) = \frac{1}{1 + \left(\frac{2.n.\sqrt{A}}{\overline{U}}\right)^{4/3}} \tag{9}$$

According to Holmes (Holmes 2001), in a frequency domain analysis for very tall tower structures, it is this latter function that takes into account the non-simultaneous occurrence of fluctuations of wind velocity. It is explicitly stated that: "*For larger structures, the velocity fluctuations do not occur simultaneously over the windward face and their correlation over the whole area must be considered. To allow for this effect, an aerodynamic admittance* $\chi^2(n)$ *is introduced*".

According to EC 1 for tall tower structures with the shape and conditions equivalent to the case study under consideration, the parameters of the spectral density function for calculating the structural factor should be determined for a reference height of approximately 0.6 of the height of the structure. Given this indication, for generating different sets of time series the height chosen was 90 meters that is about 60% of the height of lattice wind tower.

The applied wind generated forces were obtained through Eq. (7) taking into account the acting dynamic pressures and the influence area for each floor, considering the mean wind velocity depending on the height and the fluctuation velocities given by the random series generated (Ferreira 2011). Supporting the procedure used in Ferreira *et al.* (Ferreira 2011), appropriate simplifications were performed so that the wind power

spectrum was multiplied by the aerodynamic admittance; it was with this new spectrum that the turbulent velocities were calculated.

3.NUMERICAL MODEL DEVELOPMENT AND MODAL ANALYSIS

This section describes the FE software used for the analytical study. The development of the model is then discussed in detail, including selected element types, material properties and analytical concerns, damping ratio assumptions, etc.

The FE software selected to perform the three-dimensional dynamic time history analyses of the cantilevered sign and the lattice wind tower was Autodesk Robot Structural Analysis.

3.1 Cantilevered Sign Support

The development of the model resulted from previous work (Paiva 2009) (Paiva 2013), where an ultimate structural design of the cantilever support was accomplished for strength resistance (STR). The resulting work consisted in a cantilever support represented in Fig. 2, which is located somewhere in Porto district, corresponding to be situated in zone B EN 1991-1-4 of the Portugal National annex ($v_{b,0}$=30 m/s and v_b=23.1 m/s). The column and the beam have a length of 6.5 m and 6.0 m, respectively, and are constituted by a square hollow section 250*250*8 (uniform member) in steel S355. The signboard dimensions can also be seen in Fig. 2.

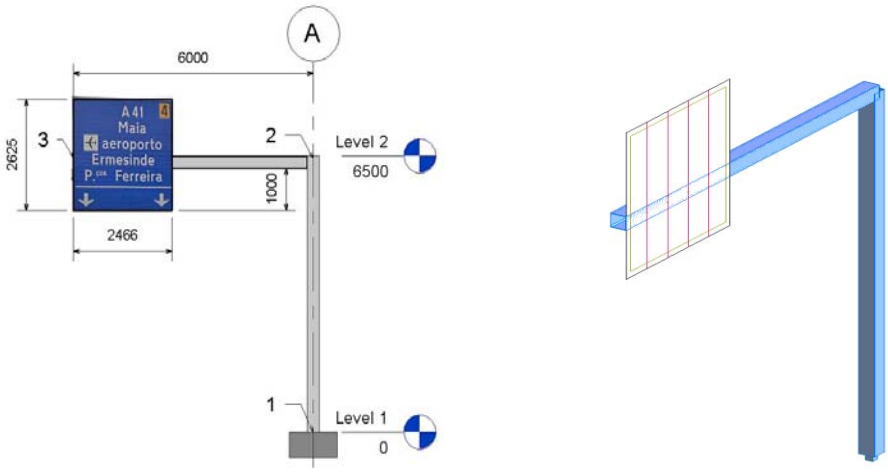

Fig. 2: Geometry of the support (dimensions in mm, left) and numerical model of the cantilever sign (right)

Two element types were used to model the different components of the structure. Three dimensional bars (beam element with tension, compression, torsion, and bending capabilities) for the column, beam and the supporting bars of the signboard. A three-dimensional elastic shell element (material aluminium) was used to model the signboard on the structure. The inclusion of the signboard characteristics on the model allows an improved capture of the dynamic behavior of the complete structure and a more direct and accurate tracking of the applied wind loads on the structure. In the time

history analyses of the structure, turbulent wind pressures are applied directly to the signboard. The mass of the structure is lumped at the structure nodal points, the masses are assumed to have only translational degree of freedom.

One final aspect of the analytical model development requires addressing the topic of damping. Damping is a very important component of most dynamic models for three main reasons. First, the level of damping within a dynamic system dictates how long the system will oscillate significantly once it has been excited. The second reason is that relatively high levels of damping (i.e. $\geq$ 20% of critical) can have a significant effect on the system's natural frequencies and mode shapes. Finally, increasing damping reduces the maximum amplitude of the oscillations (Ginal 2003).

Damping is a dynamic characteristic that is usually measured experimentally. Nevertheless, this paper has relied upon experimental field measurements of damping ratios from previous research contributions (Ginal 2003). In some research studies (Kaczinski 1998) the damping measured was "total" damping, which includes both inherent structural damping and any aerodynamic damping. Autodesk Robot Structural Analysis includes damping in its dynamic time history analysis application, through the classic formulation of Rayleigh damping with user-defined quantities. A target damping ratio equal to ξ=0,5 % was used for every mode of vibration.

In the following modal analysis only the first four modes are discussed (Fig. 3). The first mode was horizontal out-plane mode (along the wind direction), the second a vertical in-plane mode of vibration, the third was again a horizontal in-plane mode but with more expressive horizontal component and finally the fourth was an out-of-plane "twisting" mode. The first mode (in particular) and the fourth mode (Table 1) contribute to the response in y direction (along wind direction).

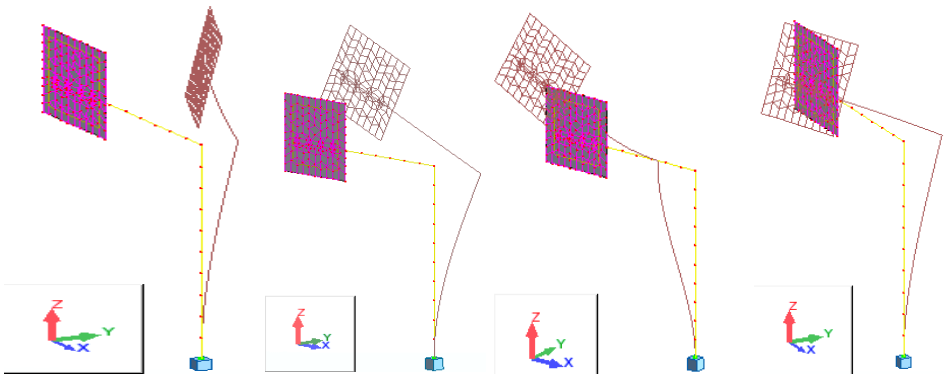

Fig. 3: First, second, third and fourth modes of vibration (from left to right) for the numerical model

Table 1: Natural frequencies and modal mass from the modal analysis

Mode	*f* (Hz)	m_y=952 (kg)	m_x=952 (kg)	m_z=952 (kg)
1	1,50	619	-	-
2	1,73	-	342	267
3	4,98	-	476	190
4	5,45	172	-	-

From this set of vibration modes (Fig. 3) some specific characteristics were observed. Also, from the pictorial display of the fifth through the tenth mode of vibration, typically show excitation of vibrational modes of the signboard and not of the supporting structure.

The remainder of this paper is devoted to the numerical study of the sign support responses, under series of wind time histories, and subsequent passive vibration control measures. In the finite element analyses of the sign support structure, the wind pressures were only applied to the surface of the sign board. Pressures were not applied to the individual members of the supporting structure. This decision was taken by considering the following two aspects.

3.2 Lattice Wind Tower

The structure chosen was a tall lattice wind tower, whose design resulted from academic studies of the authors of this paper (Henriques 2012) and is represented in Fig. 4. The tower has 150 m of height and the turbine used is FL2500 of 2.5 MW with rotor diameter of 100 m.

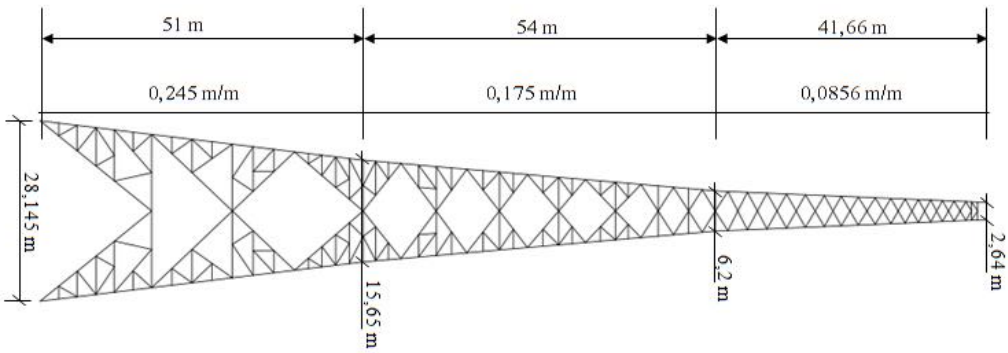

Figure 4: Tower Geometry (Henriques 2012)

The elements of the structure were disposed based on rules of triangles so as to shorten the lengths of buckling of the structural system.

The model of the tower was introduced in Autodesk Robot Structural Analysis Professional 2012, using model bars linked through rigid connections; the foundations were modeled with supports that restrict all displacements and rotations. The modeling of the wind turbine (by itself) was not performed. However were introduced bars with great rigidity and null weight to simulate the rigidity of the wind turbine on the top of the lattice tower structure. The weight of the wind turbine was considered at the top the tower by adding four vertical forces in the top of the tower with 362.60 kN each.

In this work it was considered that during the dynamic action the rotor is stopped in its most unfavorable position. The mass of the structure is lumped at the structure nodal points; the masses are assumed to have only one degree of freedom (translation in X-direction). Autodesk Robot Structural Analysis includes damping in its dynamic time history analysis application, through the classic formulation of Rayleigh damping with user-defined quantities. A target damping ratio equal to $\xi = 5\,\%$ was used for every mode of vibration.

In the modal analysis only the response from the first three modes were considered. The vibration modes are shown in Fig. 5 and the values of the natural frequencies and of the percentage of modal mass (from the total) for each vibration mode are presented in Table 2.

Table 2: Natural frequencies and percentage of modal mass, from the modal analysis

Mode	*f* (Hz)	M_x=450161,80 kg
1	0,47	53,57 %
2	2,25	25,44 %
3	3,95	14,62 %

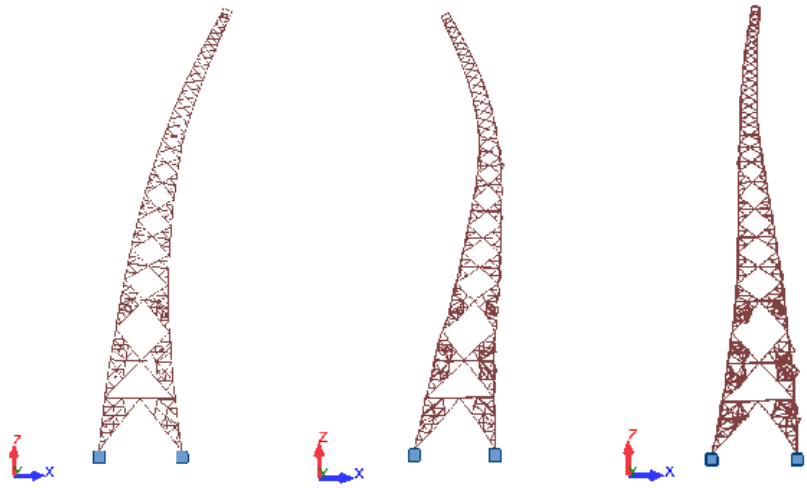

Fig. 5: First, second and third modes of vibration (from left to right) from the numerical model

3.3 Modeling a TMD for passive control of vibrations

The tuned mass dampers (TMD) can be used to control one or more vibration modes of structures excited by external actions. However, in many cases, control of the first mode is sufficient to reduce significantly the level of vibrations recorded. Except for cases in which it is intended to simultaneously monitor the contribution of more than one mode of vibration, the use of a single TMD may be satisfactory (Ferreira 2011).

The design of a TMD for application to structures without damping is universally based on two parameters – mass ratio μ and frequency ratio q – as detailed in Kelly (Kelly 1993). The optimum frequency ratio q_{opt} (corresponding to locating the fixed points at the same level or with the same displacement amplitude), the maximum amplitude of the controlled principal system, and the inherent optimal damping $\xi_{2,opt}$ of the TMD, are given by the set of Eq. (10).

$$q_{opt} = \frac{1}{1+\mu} \quad , \quad \frac{X_1}{X_{1,static}} = \sqrt{\frac{2+\mu}{\mu}} \quad , \text{ and } \quad \xi_{2,opt} = \sqrt{\frac{3\mu}{8(1+\mu)^3}} \tag{10}$$

For the design of a TMD tuned for the application to structures with damping, it is still possible to use these equations provided that the damping of the principal primary system is less or equal to 1%. For higher damping of the primary system, the use of such equations will lead to a non-optimized tuning of the TMD. For such cases, the design of the TMD can be done with design graphs (Fig 6) associated with the numerical solution of the expression giving the maximum amplitude of the controlled principal system (as used successfully in (Ferreira 2008) (Barros 2011)).

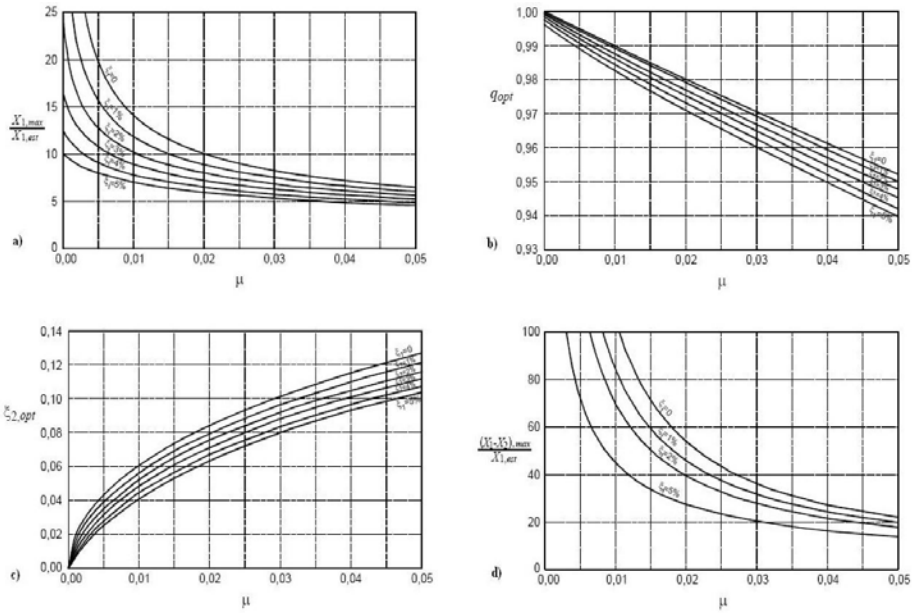

Fig. 6: Design graphs of TMD ($\xi_1 \neq 0$) (Ferreira 2008) (Barros 2011)

Kwok and Samali (Kwok 1995) also studied the behavior of a TMD in tall buildings subjected to the action of wind and, according to them, the considerations presented about the effectiveness of a TMD in response of a system of one degree of freedom can also be extended to other solid structures – such as in the case of tall buildings – leading to a modal analysis. Kwok and Samali (Kwok 1995) indicated that occurred large decreases in response for the modes controlled by the TMD's installed, while the higher order modes were not affected. For such higher modes to be also less contributive to the structural response, would require implementing new TMD's tuned according to their frequency. Thus, using modal analysis, for each vibration mode whose contribution to the overall response of the structure is important, and that one wishes to control, it is necessary to determine the corresponding values of stiffness, of mass and of modal damping (Ferreira 2011).

Since the structural software used does not have an intrinsic function that allows the direct introduction of dampers, herein for the simulation of a TMD were determined the dimensions of a square section bar with a lateral stiffness equivalent to that required for the damper placed on top. Acting as a vibrating bar (built in end – free end) with a concentrated mass that would give the frequency obtained for the sizing of the TMD with the damping introduced in the material parameters constitutive of the bar (Ferreira 2011).

Assuming a bar length L=2 m, made of steel with elasticity module E=210 GPa, from the bar stiffness $3EI/L^3$ is obtained the equivalent inertia I of the square section bar.

3.3.1 Modeling a TMD for Passive Control of Vibrations for the Cantilevered Sign

It is assumed herein, for control of vibrations purposes, that the response is solely dependent on the first vibration mode (low fundamental frequency 1.5 Hz), with which the TMD solutions were designed with the expressions available for harmonic vibration with frequency equal to the first vibration frequency of the overall structure.

Accordingly, the value of the modal mass corresponding to the first mode of vibration was determined as 619 kg and the corresponding modal stiffness as 54983,56 N/m. For the case study structure with the deployment of TMD's, only one mass ratio scenario is considered herein using μ=0.01. In Table 3 the values adopted are outlined and is also indicated the dimensions required for such bar, for the mass ratio considered in the design of the TMD.

Table 3: Optimal parameters of TMD for the support sign structure

TMD μ (mass ratio)	q_{opt}	$\xi_{TMD,opt}$	m_{TMD} (kg)	ω_{TMD} (rad/s)	k_{TMD} (N/m)	Size (cm) of square section steel bar, L=2 m
0.01	0,99	0,06	6,19	9,33	539,0	1,69*1,69

Table 4 shows the first four natural frequencies of the vibration modes of the case-study structure incorporating the TMD solution; from the table below it can be seen that the first natural frequency decreases about 8% from 1.50 Hz to 1.39 Hz, while the other frequencies remain practically constant.

Table 4: Natural Frequencies of the first four modes with TMD vibrating bar

Mode	1	2	3	4
f (Hz)	1,39	1,73	4,97	5,49

3.3.2 Modeling a TMD for Passive Control of Vibrations for the Lattice Wind Tower

Since the fundamental frequency of the tall wind tower under study is very low (0.47 Hz) and because the wind action has a spectral density function with strong content for low frequencies, it is possible that the response is conditioned by the harmonic of the fundamental frequency. For control of vibrations purposes it is assumed herein that the response is only dependent on the first vibration mode, with which the TMD solutions were designed with the expressions available for harmonic vibration with the frequency equal to the first vibration frequency of the overall structure.

Accordingly, the value of the modal mass corresponding to the first mode of vibration was determined as 126.25 ton. For the case study wind tower structure with the deployment of a TMD, only one mass ratio is herein considered $\mu = 0.01$, for which with the design charts (Fig. 6) it was possible to determine the optimal parameters to be adopted for each TMD situation. In Table 5 the values adopted are systematized.

Table 5: Optimal parameters of a TMD for the tall wind tower

TMD mass ratio μ	q_{opt}	$\xi_{TMD,opt}$	m_{TMD} (ton)	ω_{TMD} (rad/s)	k_{TMD} (kN/m)	Size (cm) of square section steel bar, L=2 m
0.01	0.987	0.046	1.7626	2.915	14.974	3.89

Table 6: Natural Frequencies of the first four modes of wind tower with TMD

Mode	1	2	3	4
f (Hz)	0,45	0,49	2,25	3,95

Table 6 shows the first four natural frequencies of the vibration modes of the case-study wind tower structure incorporating the TMD solution.

4. DYNAMIC WIND ANALYSIS OF THE TWO STRUCTURES WITH AND WITHOUT USING A TMD FOR PASSIVE CONTROL OF VIBRATIONS

4.1 Cantilevered Sign Support

Based on the methodology adopted for consideration of the dynamic wind action (using a set of 10 time series, for frequencies within the wind spectral density function evaluated with 1000 frequency intervals), the results in terms of displacements and accelerations have been evaluated and compared for the computational structural model, without and with installed TMD vibrating bar.

Using the mentioned structural software with modal superposition, a damping ratio of 0.5 percent and an integration time step of Δt=0.06 sec, ten series of wind dynamic loads were applied and their average results obtained in terms of displacements and accelerations. Fig. 7 and 8 show the time variations of acceleration and displacement on the tip of the beam (node 3, in Fig.2) of the sign support, for the wind pressure evaluated using Eq. (7), with velocity fluctuations corresponding to wind series 1.

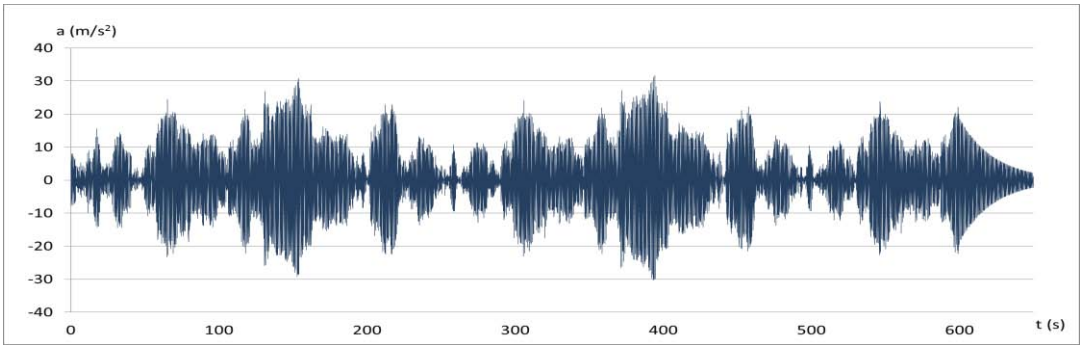

Fig. 7: Accelerations of node 3 of the beam, for wind loads corresponding to wind series 1

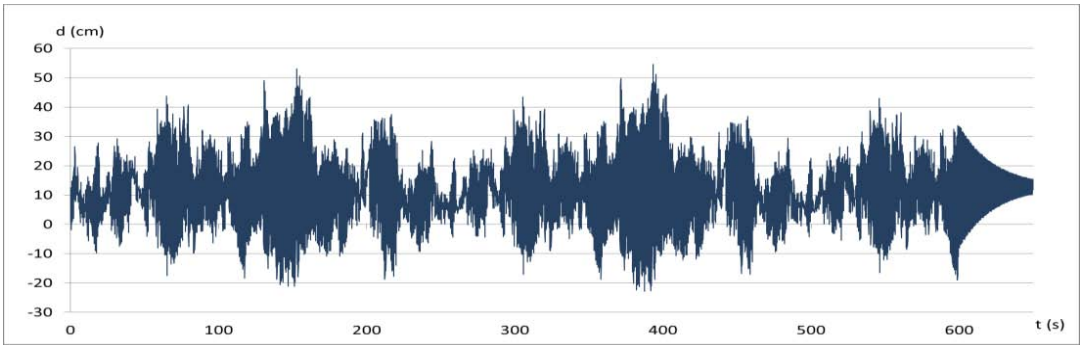

Fig. 8: Displacements of node 3 of the beam, for wind loads corresponding to wind series

Table 2: Maximum displacements and accelerations on node 3, for each of the wind time series (without TMD)

Series	1	2	3	4	5	6	7	8	9	10	Average
Max displacement (cm)	54,5	46,4	53,9	66,2	53,3	53,2	55,0	62,4	58,4	61,2	56,4
Max acceleration (m/s^2)	31,6	27,4	31,1	40,0	27,4	34,2	35,6	36,4	27,6	33,3	32,4

Fig. and Fig. show the time variations of acceleration and displacement on the tip of the beam (node 3, in Fig. 2) of the support sign, equipped with the TMD modeled with mass ratio of 1%, for wind loads evaluated using Eq. (7) and with velocity fluctuations corresponding to wind series 1.

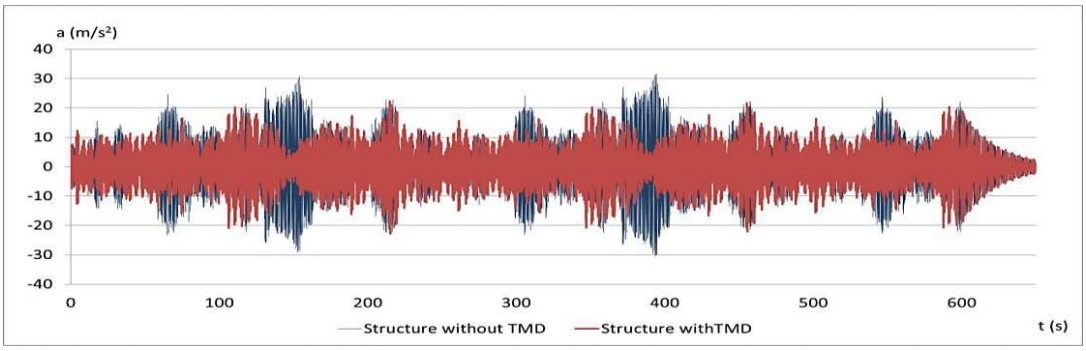

Fig. 9: Accelerations of node 3 of the beam, equipped with the TMD modeled with mass ratio of 1% for wind loads corresponding to wind series 1

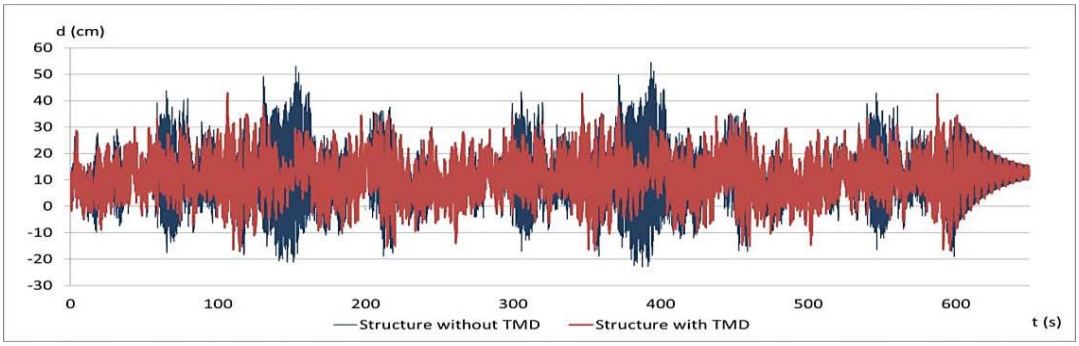

Fig. 10: Displacements of node 3 of the beam, equipped with the TMD modeled with mass ratio of 1% for wind loads corresponding to wind series 1

Table 5 presents a summary of maximum values of displacements and accelerations on node 3 of the structure, for each of the time series.

Table 3: Maximum displacements and accelerations on node 3, for wind time series (TMD mass ratio μ=0,01)

Series	1	2	3	4	5	6	7	8	9	10	Average
Max displacement (cm)	43,0	40,9	48,1	53,5	50,6	45,7	40,3	40,7	49,7	45,0	45,8
Max acceleration (m/s^2)	22,8	23,5	27,4	29,4	28,3	22,8	21,6	22,1	23,3	23,9	24,5

The efficiency of using the modeled TMD on the structure can be interpreted by the results of Table 6, here associated with mass ratio of 1%. In this design case it was observed a reduction of maximum displacements and accelerations in the order of 20% and 25%, respectively.

Table 6: Efficiency of using the modeled TMD for mass ratio of 1%

	Structure Without TMD	Structure With TMD (μ=0.01)	Reduction relative to structure without TMD
Maximum displacement (cm)	56,4	45,8	19 %
Maximum acceleration (m/s^2)	32,4	24,5	24 %

4.2 Lattice Wind Tower

The same procedure is done for the lattice tower, but in this case using a set of 4 time series, for the dynamic wind action. Recurring to the mentioned structural software with modal superposition, a damping ratio of 5 % and an integration time step of $\Delta t = 0.2$ seconds, the four series of wind dynamic loads were applied and their average results obtained in terms of top displacements and accelerations. As an example, Fig.

11 and Fig. 12 show the time variations of top acceleration and displacement of the wind tower for the wind loads evaluated using equation (7), with velocity fluctuations corresponding to wind series 1. Table 7 presents a summary of maximum values of tower top displacements and accelerations, for each of the time series.

Table 7: Maximum displacements and accelerations on node 3, for each of the wind time series (without TMD)

Series	1	2	3	4	Average
Maximum displacement (cm)	70,39	66,07	68,99	65,77	67,80
Maximum acceleration (cm/s^2)	184,15	179,49	179,89	222,36	191,47

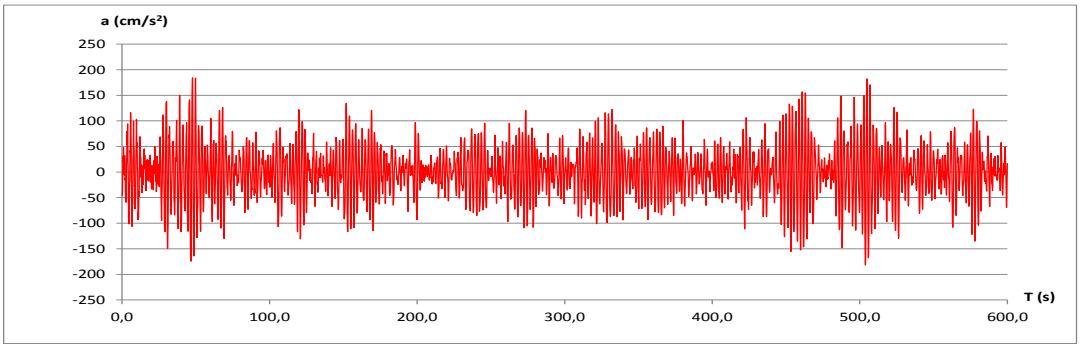

Fig. 11: Accelerations on top of tower, for wind loads corresponding to wind series 1

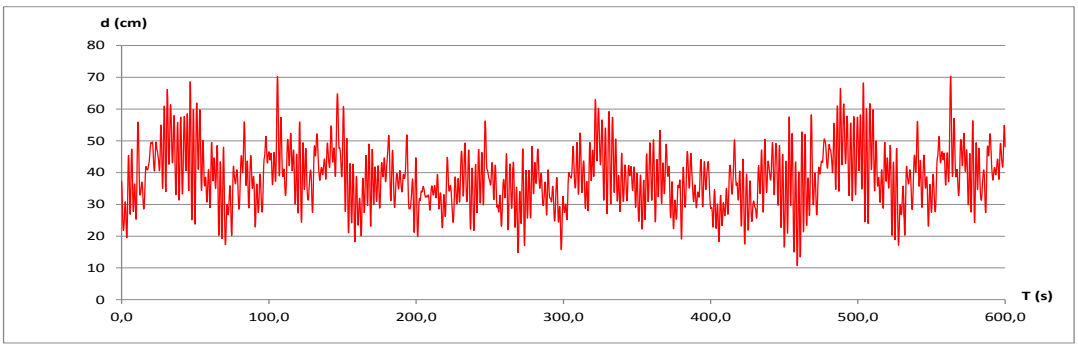

Fig. 12: Displacements on top of tower, for wind loads corresponding to wind series 1

As regards to the use of a TMD on the top of the wind tower, as used in (Ferreira 2011) in an earlier comparison associated with a tall structure subjected to harmonic excitation in resonance with the fundamental frequency, the Fig. 13 show such comparison of top displacements and accelerations of the given tall wind tower along the time, without and with TMD with mass ratio of 1 %. As can be seen in Fig. 13, if the structure is acted upon by a harmonic action in resonance with fundamental frequency, the implementation of the TMD can considerably attenuate the response of the wind tower structure.

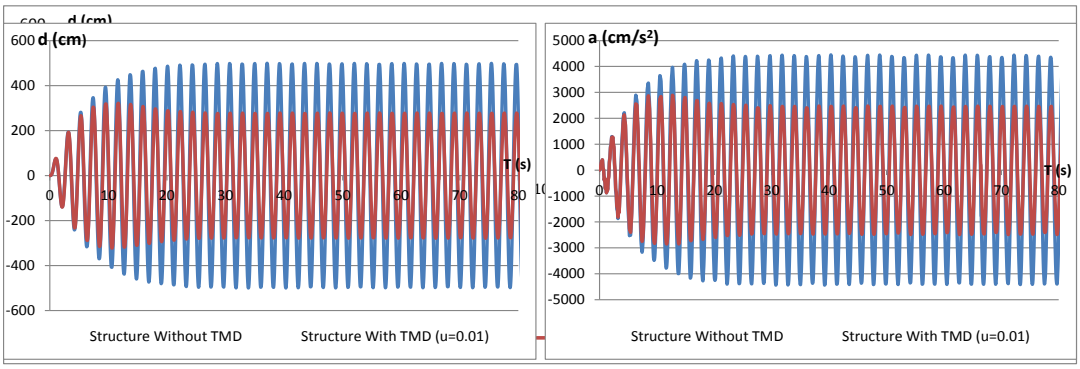

Fig. 13: Top displacements (left) and accelerations (right), under a harmonic fundamental resonant excitation, without and with TMD

Fig. 14 and Fig. 15 show the time variations of top acceleration and displacement of the wind tower, equipped with the TMD modeled before with a 1% mass ratio, for the wind loads evaluated using Eq. (7), with velocity fluctuations corresponding to wind series 1. Table 8 presents a summary of maximum values of top displacements and accelerations of the tower, for each of the time series. It also presents the average of such maximum values.

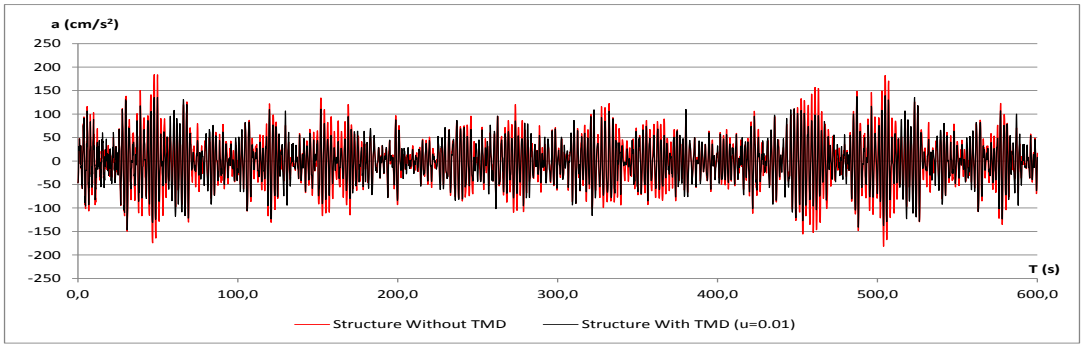

Fig. 14: Acceleration on the top of tower, equipped with the TMD modeled with mass ratio of 1 % for the wind loads corresponding to wind series 1

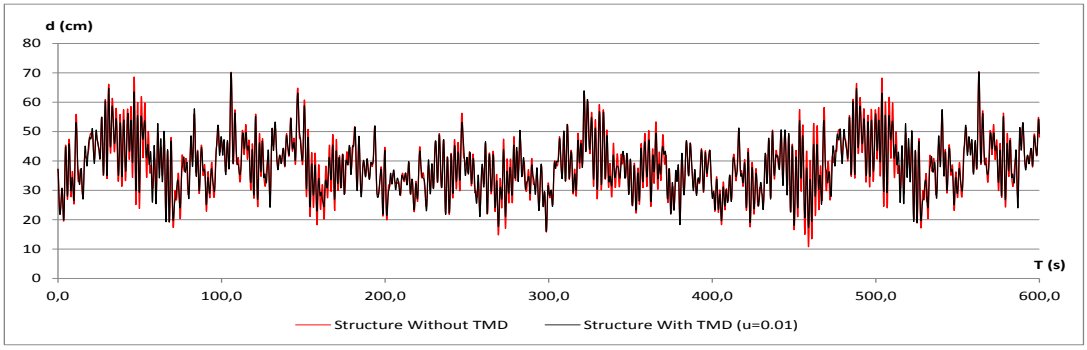

Fig. 15: Displacement on the top of tower, equipped with the TMD modeled with mass ratio of 1 % for the wind loads corresponding to wind series 1

Table 8: Maximum displacements and accelerations on node 3, for each of the wind time series (with TMD)

Series	1	2	3	4	Average
Maximum displacement (cm)	70,30	63,42	70,62	63,96	67,07
Maximum acceleration (cm/s^2)	139,35	151,72	156,57	180,69	157,08

The efficiency on the use of the modeled TMD in the tower structure can be interpreted by the results of Table 9, here associated with a mass ratio of 1%: reduction of top maximum displacements and accelerations on the order of 1% and 18%, respectively.

Table 9: Efficiency of using the modeled top TMD for mass ratio of 1%

	Structure without TMD	Structure with TMD (u=0.01)	Reduction (%) in relation to the structure without TMD
Maximum displacement (cm)	67,80	67,07	1 %
Maximum acceleration (cm/s^2)	191,47	157,08	18 %

5. CONCLUSIONS

This work summarizes a set of wind effects that the studied structures are subjected. The paper than introduces and describes a method for simulating series of wind histories for in-service behavior. The numerical models used in the present study, suggests that both models will be able to capture important aspects of the dynamic response of the structures.

5.1 Cantilevered Sign Support

For the case of cantilevered sign support the present study only evaluated the structural response of the cantilevered sign support to natural wind gusts applied in the frontal surface of the signboard (out-of-plane behavior). The actual model provides a solid foundation for a possible subsequent fatigue evaluation of this structure. A few remarks are made on the damping in the structure. Since in this work the TMD implementation was only considered for vibrations in the out-of-plane direction (induced by natural wind), future studies should also focus in ways to provide effective damping in both directions. In fact efforts should be made in the developing of a combination of two damping devices, taking into account the possible combination of galloping, natural wind and truck gust of the cantilever signs supports. From a structural system perspective, the in-plane and the out-of-plane behaviors are almost uncoupled (modes of vibration); hence the movement (and suppression) can be considered independently and superimposed. Further studies should also reflect the details needed for the practical implementation of the TMD, considering the great flexibility required. Regarding the implementation of the TMD, it was concluded that this device is proving

to be effective in reducing displacements and accelerations, when the structure is subjected to the artificially generated natural wind. For the TMD modeled with the parameters calculated, it was concluded that in terms of maximum accelerations reductions of the order of 24% can be achieved for a TMD with 1% mass ratio. In terms of maximum displacements it was also concluded that the structural reference system has proved less effective, achieving reductions of 19% for a TMD with 1% mass ratio.

5.2 Lattice Wind Tower

The simplified methodology adopted for the evaluation of the effects of the dynamic wind action, consisted of varying forces over time at each stiffening floor, following the same law of variation. This law is obtained, for each generated time series, from the Eurocode 1 wind power spectrum multiplied by the aerodynamic admittance function. As regards to the implementation of the TMD in the tall wind tower structure under study, it was concluded that it proved to be very effective in terms of both top displacements and top accelerations, when the tower is subject to a harmonic action in resonance with fundamental frequency of vibration of the tower. The application of this TMD passive device on top of the tower for vibration control of the designed wind tower, subjected to natural wind actions based on the generated wind series, is not as effective as for controlling harmonic resonant phenomena. With the implementation of the TMD it was concluded that this device is considerably more effective in controlling top accelerations (rather than top displacements), when the structure is subjected to the artificially generated natural wind. For the TMD modeled with the parameters calculated, were observed maximum accelerations reductions of the order of 18%, while the achieved reduction of maximum displacements was only of the order of 1%.

ACKNOWLEDGMENTS

This work was co-participated by funds from the project “VHSSPOLES-Very High Strength Steel Poles” (Faculty of Engineering of the University of Porto, reference 21518) sponsored by the European Fund for Regional Development (FEDER) through COMPETE (Operational Program Competitiveness Factors - POFC). The Authors acknowledge the financial support and the opportunity to contribute to the development of the transmission towers testing site of Metalogalva (Trofa, Portugal).

REFERENCES

Barros, J.E. and Moutinho, C. and Barros, R.C. (2011) “The use of TMD’s with heavy mass to mitigate the seismic response of structures.” *Proceedings of 3rd ECCOMAS Thematic Conference on Computational Methods in Structural Dynamics and Earthquake Engineering (COMPDYN 2011)*, Corfu, Greece.

Davenport, A.G. (1961), “The Spectrum of Horizontal Gustiness Near the Ground in High Winds.” *Journal of the Royal Meteorological Society, Vol.* ***87****, 194-211.*

Dexter, R.J. and Johns, K. W. (2005), “The Development of Fatigue Design Load Ranges for Cantilevered Sign and Signal Support Structures” *Journal of Wind Engineering, Vol.* ***77****, 315-325.*

EN 1991-1-4. Eurocode 1: actions on structures, general actions. Part 1-4, Wind actions, CEN, Brussels; April 2005

Ferreira, N.A.C. and Barros, R.C. and Delgado, R. (2011), *Proceedings of 3rd ECCOMAS Thematic Conference on Computational Methods in Structural Dynamics and Earthquake Engineering (COMPDYN 2011),* Corfu, Greece.

Ginal, S. (2003), "Fatigue Performance of Full-Span Sign Support Structures Considering Truck-Induced Gust and Natural Wind Pressures" M.Sc. Thesis, Faculty of the Graduate School, Marquette University

Henriques, J.M. (2012), "Projecto de torres eólicas reticuladas de grande altura (150m): Modelação e análise comparativa com estruturas tubulares auto-suportadas." M.Sc. Thesis in Structural Engineering, Faculdade de Engenharia da Universidade do Porto (FEUP), Porto, Portugal

Henriques, J (2013), "Design of Lattice Wind Towers and Comparison with the Typical Self-Supported Tubular Towers" *Proceedings of 4th International Conference on Integrity, Reliability & Failure,* Funchal, Portugal

Holmes, J.D. (2001), *Wind Loading of Structures*, Spon Press, London

Iannuzzi, A. and Spineli, P. (1987), "Artificial Generation and Structural Response." *Journal of Structural Engineering, Vol.* ***113****(2), 2382–2398.*

Kaczinski, M.R. and Dexter, R.J. and Van Dien, J.P. (1998), "Fatigue Design of Cantilevered Signal, Sign and Light Supports", NCHRP Report 412, Transportation Research Board, Washington, D.C.

Kwok, K. and Samali, B. (1995), "Performance of tuned mass dampers under wind loads" Engineering Structures, Vol. **17**(9), 655-667.

Lee, C.L. and Chen, Y.T and Chung, L.L. and Wang Y.P. (2006) "Optimal design theories and applications of tuned mass dampers" *Engineering Structures, Vol.* ***28****(1), 45-53.*

Madugula, M.K.S. (2002), Dynamic Response of Lattice Towers and Guyed Masts. Structural Engineering Institute, American Society of Civil Engineers (ASCE), Reston VA

Paiva, F.M. (2009), "Análise e dimensionamento de pórticos metálicos de sinalização em Auto-Estradas." M.Sc. Thesis in Structural Engineering, Faculdade de Engenharia da Universidade do Porto (FEUP), Porto, Portugal

Paiva, F. and Barros, R.C. (2013), "Analysis of the stability and design of cantilevered sign supports in highways" *Proceedings of 4th International Conference on Integrity, Reliability & Failure,* Funchal, Portugal

Scanlan, R.H. and Simiu, E. (1986), *Wind Effects on Structures,* 2nd Edition. Wiley-Interscience, New York

Vickery, B.J. and Kao, K.H. (1972) "Drag of Along-Wind Response of Slender Structures." *Journal of Structural Division, ASCE, Vol.* ***98****(1), Proc. Paper 8635, 21-36, New York*